Hindawi Publishing Corporation
EURASIP Journal on Wireless Communications and Networking
Volume 2009, Article ID 315765, 10 pages
doi:10.1155/2009/315765

Research Article

Blind CP-OFDM and ZP-OFDM Parameter Estimation in Frequency Selective Channels

Vincent Le Nir (EURASIP Member),[1] Toon van Waterschoot,[1] Marc Moonen (EURASIP Member),[1] and Jonathan Duplicy[2]

[1] *ESAT/SISTA Laboratory, Department E.E., Katholieke Universiteit Leuven, Kasteelpark Arenberg 10, 3001 Leuven-Heverlee, Belgium*
[2] *Agilent Technologies Labs, WingePark 51, 3110 Rotselaar, Belgium*

Correspondence should be addressed to Vincent Le Nir, vincent.lenir@esat.kuleuven.be

Received 14 November 2008; Revised 4 March 2009; Accepted 1 June 2009

Recommended by A. Lee Swindlehurst

A cognitive radio system needs accurate knowledge of the radio spectrum it operates in. Blind modulation recognition techniques have been proposed to discriminate between single-carrier and multicarrier modulations and to estimate their parameters. Some powerful techniques use autocorrelation- and cyclic autocorrelation-based features of the transmitted signal applying to OFDM signals using a Cyclic Prefix time guard interval (CP-OFDM). In this paper, we propose a blind parameter estimation technique based on a power autocorrelation feature applying to OFDM signals using a Zero Padding time guard interval (ZP-OFDM) which in particular excludes the use of the autocorrelation- and cyclic autocorrelation-based techniques. The proposed technique leads to an efficient estimation of the symbol duration and zero padding duration in frequency selective channels, and is insensitive to receiver phase and frequency offsets. Simulation results are given for WiMAX and WiMedia signals using realistic Stanford University Interim (SUI) and Ultra-Wideband (UWB) IEEE 802.15.4a channel models, respectively.

1. Introduction

Spectral monitoring has received considerable attention in the context of opportunistic and cognitive radio systems. Blind modulation recognition (with no a priori information) consists in identifying the different signal components (air interfaces) that are present in an observed spectrum. A survey of algorithms currently available in literature can be found in [1]. While past studies have focused on single-carrier modulations, research has recently also focused on the identification of multicarrier modulations. On one hand, mixed moments [2] and fourth-order cumulants [3, 4] can be used to discriminate between single-carrier and multicarrier modulations and to estimate their parameters. For instance, the fourth-order cumulants of OFDM signals converge to 0 as the number of subcarriers increases independently of the Signal-to-Noise Ratio (SNR) and hence can be used to distinguish between single-carrier modulations and multicarrier modulations propagating through an Additive White Gaussian Noise (AWGN) channel. Unfortunately, mixed moments and fourth-order cumulants do not perform well for more realistic channels, that is, frequency selective channels with time and frequency offsets. On the other hand, cyclic autocorrelation-based features [5–7] have been proposed to discriminate between single-carrier and multicarrier modulations in time dispersive channels and affected by AWGN, carrier phase, and time and frequency offsets.

Moreover, a number of procedures [8–11] have been proposed using autocorrelation- and cyclic autocorrelation-based features to extract parameters for OFDM signals using a Cyclic Prefix time guard interval (CP-OFDM) and propagating through a frequency selective channel. In this paper, we review the existing techniques presented in [5–12] using autocorrelation- and cyclic autocorrelation-based features for CP-OFDM signals in frequency selective channels to determine the power, oversampling factor, useful time interval, cyclic prefix duration, number of subcarriers, and time and frequency offsets. The carrier frequencyof the signal of interest is first estimated by an energy detector in the spectral domain followed by a downconversion to baseband for further analysis. Then, we propose a blind parameter estimation technique based on a power autocorrelation feature which can be operated in frequency selective

channels and applied to OFDM signals using a Zero Padding time guard interval (ZP-OFDM). The zero padding, in particular, excludes the use of the autocorrelation- and cyclic autocorrelation-based techniques. The proposed technique leads to an efficient estimation of the symbol duration and zero padding duration, and it is insensitive to phase and frequency offsets.

In Section 2, we review the blind parameter estimation using features based on autocorrelation and cyclic autocorrelation for CP-OFDM signals. In Section 3, we present the blind parameter estimation using a new feature based on power autocorrelation for ZP-OFDM signals. Simulation results are given in Section 4 for WiMAX and WiMedia signals using realistic Stanford University Interim (SUI) and Ultra Wide-Band (UWB) IEEE 802.15.4a channel models respectively [13, 14].

2. Blind Parameter Estimation Using Features Based on Autocorrelation and Cyclic Autocorrelation

In this section, we review different algorithms used for the estimation of the carrier frequency, power, and oversampling factor of an observed signal component. Then the features based on autocorrelation and cyclic autocorrelation are presented for CP-OFDM signals to estimate the useful time interval, cyclic prefix duration, and the number of subcarriers in frequency selective channels.

2.1. Estimation of the Carrier Frequency. To estimate the carrier frequencies f_c^i, $i = 0 \cdots N_s - 1$ with N_s the number of signals components present in an observed spectrum, one can use a nonparametric approach based on a Fast Fourier Transform (FFT) [12]. This method is appropriate for narrowband signals above the noise floor provided that the frequency resolution is high enough. One can assume that the observed compound signal has been sampled at least twice the maximum bandwidth of interest :

$$\mathbf{S} = |\mathrm{FFT}(\mathbf{s})|^2 \tag{1}$$

with $\mathbf{s}$ the received sampled data stream $\mathbf{s} = [s(0) \cdots s(N' - 1)]^T$ and $\mathbf{S}$ its Power Spectral Density (PSD) (N' is the number of samples). Note that the larger the number of samples, the higher the frequency resolution provided by the FFT grid. This is a crucial parameter to detect signals having a small bandwidth. However, if the FFT size is too large, the sequence of length N' can be divided into M blocks of size T, then one can perform M FFTs of length T and add the contribution of each block given by (1). The carrier frequencies f_c^i, $i = 0 \cdots N_s - 1$ are then estimated by detecting the band-edges B_{low}^i and B_{high}^i, for all $i = 0 \cdots N_s - 1$ with a threshold between the noise level and the signal level, which is driven by thesensitivity of the receiver. The carrier frequencies are then estimated as

$$f_c^i = \frac{B_{\mathrm{low}}^i + B_{\mathrm{high}}^i}{2}, \quad i \in [0 \cdots N_s - 1]. \tag{2}$$

2.2. Estimation of the Oversampling Factor and Power Spectral Density. Assuming that the carrier frequencies have been estimated, then each individual signal component of interest can be downconverted to baseband and lowpass filtered (with decimation). The resulting digital baseband signal can then be modeled as a received sequence $\mathbf{y} = [y(0) \cdots y(N-1)]^T$ of length N such that

$$y(i) = e^{j(2\pi\epsilon i + \phi)} \sum_{l=0}^{L-1} h(l)x(i-l) + n(i), \quad i \in [0 \cdots N-1], \tag{3}$$

where $\mathbf{x} = [x(0) \cdots x(N-1)]^T$ is the vector of N transmitted symbols, which have been oversampled by a factor q, the $h(l)$'s are the multipath channel coefficients with L the number of channel taps, $\mathbf{n} = [n(0) \cdots n(N-1)]^T$ is the vector of Additive White Gaussian Noise (AWGN), ϕ is the receiver phase offset, and ϵ is the receiver frequency offset.

In order to calculate the oversampling factor q, which corresponds to the ratio between the bandwidth of the lowpass filter and the bandwidth of the signal of interest, one can use again a nonparametric approach based on a Fast Fourier Transform (FFT) on the received sequence [11]:

$$\mathbf{Y} = |\,\mathrm{FFT}(\mathbf{y})\,|^2 \tag{4}$$

with $\mathbf{Y}$ the PSD of the received signal. Then, the idea is to design a target filter $\mathbf{Y}^{\mathrm{target}}$ which has the smallest Euclidian distance to $\mathbf{Y}$. Knowing the total energy $A = \mathrm{sum}(\mathbf{Y})$ in the frequency domain, one can design the following target filter:

$$\mathbf{Y}_i^{\mathrm{target}} = \left[\frac{A}{2i}\mathrm{ones}(i), \mathrm{zeros}(N-2i), \frac{A}{2i}\mathrm{ones}(i)\right]^T \tag{5}$$

with $\mathrm{ones}(i)$ the all-one vector of length i and $\mathrm{zeros}(i)$ the all-zero vector of length i. The optimization problem is to minimize over i the following expression:

$$i_{\mathrm{opt}} = \min_i \left(\mathbf{Y} - \mathbf{Y}_i^{\mathrm{target}}\right)^2. \tag{6}$$

An exhaustive search on the index i is performed to solve this optimization problem. Then, one can calculate the ratio q between the bandwidth of the lowpass filter and the bandwidth of the signal of interest. The number of FFT points spanning the bandwidth of the lowpass filter corresponds to the number of samples N, while the number of FFT points spanning the transmitter bandwidth corresponds to twice the cutoff frequency of the optimal target filter. Once the optimal i_{opt} is found, one can calculate the oversampling factor:

$$q = \frac{N}{2i_{\mathrm{opt}}}. \tag{7}$$

The estimated signal power (average of PSD over all frequency bins) p is then defined as

$$p = \frac{A}{2i_{\mathrm{opt}}}. \tag{8}$$

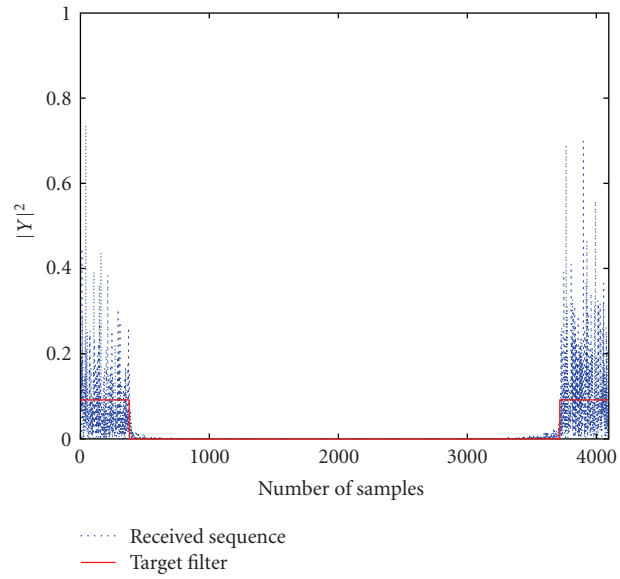

Figure 1: Estimation of the oversampling factor and power spectral density using real world measurement data.

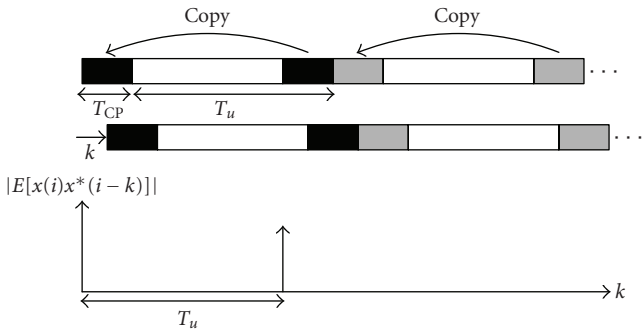

Figure 2: Correlation on a CP-OFDM signal.

Figure 1 shows an example of a received sequence of 4096 samples from a real CP-OFDM data measurement (with 26 tones going through an unknown channel and sampled at the receiver with a known sampling rate) after carrier estimation, downconversion, and lowpass filtering. The estimation of the oversampling factor and signal power is performed using the algorithm presented in this section, leading to $q = 5.1$ and $p = 0.12$ for this particular data measurement.

2.3. Estimation of the Useful Time Interval and the CP-Length for CP-OFDM Signals. The estimation of the useful time interval T_u and the CP-length T_{CP} exploits autocorrelation or cyclic autocorrelation properties of the received sequence [9–11]. The autocorrelation of the received sequence which corresponds to the second-order/one-conjugate cyclic cumulant at zero cyclic frequency in the work of [6, 7] can be written as

$$r(k) = \frac{1}{N}\sum_{i=0}^{N-1} y(i)y^*(i-k), \quad k \in [0 \cdots N-1] \tag{9}$$

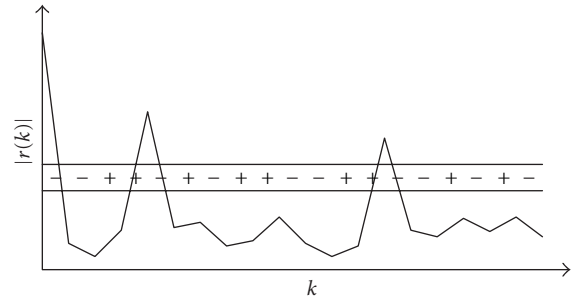

Figure 3: Peak detection algorithm based on positive and negative slopes.

with k the shift index. One can assume that the autocorrelation function is cyclically shifted; that is, two vectors $\mathbf{y}$ are concatenated in order to cope with the data outside the interval $i \in [0, N-1]$. For CP-OFDM, the last part of the OFDM symbol is copied at the beginning to prevent Inter Symbol Interference (ISI) after multipath propagation. Therefore, a peak in the autocorrelation function can be observed at delay T_u. Figure 2 shows the ideal autocorrelation function for a transmitted CP-OFDM signal $x(i)$.

The autocorrelation function can be derived by replacing the received sequence model (3) into (9), leading to

$$r(k) = \begin{cases} \sum_{l=0}^{L-1} |h(l)|^2\sigma_x^2 + \sigma_n^2, & k = 0, \\ e^{j2\pi\epsilon T_u}\sum_{l=0}^{L-1} |h(l)|^2 \frac{T_{CP}}{T_s}\sigma_x^2, & k = T_u, \\ e^{j2\pi\epsilon k}\sum_{l=0}^{L-1} h(l+k)h^*(l)\sigma_x^2, & k = 1,\ldots,L-1, \\ e^{j2\pi\epsilon k}\sum_{l=0}^{L-1} h(l+k-T_u) & \\ \qquad \times h^*(l)\frac{T_{CP}}{T_s}\sigma_x^2, & k = T_u + (1,\ldots,L-1), \\ 0, & \text{otherwise} \end{cases} \tag{10}$$

with σ_x^2 the variance of the transmitted signal and σ_n^2 the variance of the AWGN. As stated by these equations, there are $2L$ peaks due to the multipath coefficients when the channel is stationary over the observation window. Therefore, one can use a peak detection algorithm similar to [7] based on positive and negative slopes ("+−" corresponding to the event of a positive slope followed by a negative slope on Figure 3). One can assume that the maximum channel delay spread L is smaller than the useful time interval T_u, and therefore the peaks corresponding to the cyclic prefix insertion will appear as a second cluster of peaks at higher values of k. Hence one can discard the peaks with the lowest shifts and keep the peaks with the highest shifts for the estimation of the useful time interval.

Figure 3 shows the technique used for estimating the largest peak. The useful time interval $T_u = k_{opt}$ is estimated

by an exhaustive search according to the following optimization problem:

$$k_{\text{opt}} = \max_{k>L}(|r(k,+-\text{occurs})| - |r(k,\text{previous}-+)|) \tag{11}$$

corresponding to the search for the optimal index k for which the difference between a peak (when a $+-$ occurs) and its lowest previous point (its previous $-+$) is maximized. The choice of the modulus $|\cdot|$ leads to an insensitivity of the autocorrelation feature to phase and frequency offsets (as the exponentials factors in (10) disappear).

The number of subcarriers N_c can be determined as the ratio between the useful time interval T_u and the transmitter sampling period T_t [11]. Moreover, the ratio between the transmitter sampling period and the sampling period of the lowpass filter T_r leads to the oversampling factor $q = T_t/T_r$. Without loss of generality, the sampling period of the lowpass filter T_r is normalized to unity. Therefore, once the useful time interval T_u has been estimated, one can determine the number of subcarriers by

$$N_c = \frac{T_u}{q}. \tag{12}$$

From [8], it is known that a CP-OFDM signal is cyclostationary with period $T_s = T_u + T_{\text{CP}}$. The cyclic autocorrelation is given by

$$C^{\beta}(k) = \frac{1}{N}\sum_{i=0}^{N-1} y(i)y^*(i-k)e^{-2\pi j\beta i/N}, \quad (k,\beta) \in [0\cdots N-1]. \tag{13}$$

From the model in (3), one can determine the cyclic period T_s using the following optimization problem with an exhaustive search on β:

$$\beta_{\text{opt}} = \max_{\beta\neq 0}\left|C^{\beta}(T_u)\right|^2. \tag{14}$$

The cyclic period can then be found by the following equation:

$$T_s = T_u + T_{\text{CP}} = \frac{N}{\beta_{\text{opt}}}. \tag{15}$$

Finally, time and frequency offsets can be determined using cyclostationarity properties of CP-OFDM signals with prior information on the pulse shaping filter [8] or conventional autocorrelation methods without prior knowledge on the pulse shaping filter [15].

3. Blind Parameter Estimation Using a Feature Based on Power Autocorrelation

ZP-OFDM signals differ from CP-OFDM signals in that zeros are appended at the end of each OFDM symbol (instead of a CP for the next symbol). Therefore ZP-OFDM signals exhibit neither autocorrelation nor cyclic autocorrelation properties. To estimate the symbol duration T_s, we introduce a new feature which will be referred to as "power autocorrelation." The power autocorrelation feature can be also referred to the fourth-order/two-conjugate moment at delay vector $[0, 0, -k, -k]$ [7]. Moreover, this feature will be used to estimate the zero padding duration T_{ZP}. The power autocorrelation feature is defined as

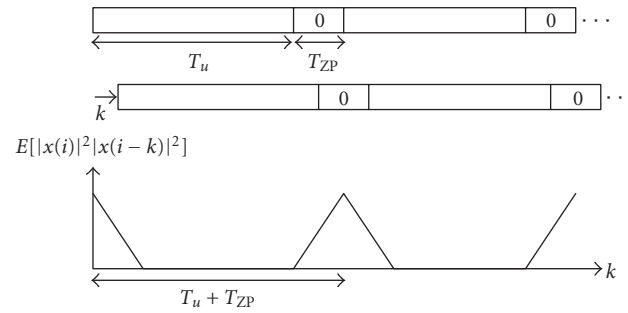

Figure 4: Power autocorrelation on a ZP-OFDM signal.

$$d(k) \triangleq \frac{1}{N}\sum_{i=0}^{N-1} |y(i)|^2 |y(i-k)|^2, \quad k \in [0\cdots N-1] \tag{16}$$

with k the shift index and where $y(i)$ is defined in (3). By autocorrelating the power of the transmitted sequence, we can observe a train of triangles with period T_s as shown in Figure 4.

We define $c = |k - tT_s|$ as the absolute value of the timing difference between the shift index k and an integer multiple t of the symbol duration T_s. The integer multiple t correspond to a train index as the received power sequence is a cyclic function with period T_s. By substituting (3) in (16), the values of the power autocorrelation are given by

$$d(k) = \begin{cases} \dfrac{T_u}{T_s}\left(\sum_{l=0}^{L-1}|h(l)|^4\mu_x^4 + 4\sigma_x^2\sigma_n^2 + \mu_n^4\right) + \dfrac{T_{\text{ZP}}}{T_s}\mu_n^4, \\ \qquad\qquad k,t=0 \\ \dfrac{T_u - c}{T_s}\left(\sum_{l=0}^{L-1}|h(l)|^2\sigma_x^2 + \sigma_n^2\right)^2 \\ \quad + \dfrac{2c}{T_s}\sigma_n^2\left(\sum_{l=0}^{L-1}|h(l)|^2\sigma_x^2 + \sigma_n^2\right) + \dfrac{T_{\text{ZP}} - c}{T_s}\sigma_n^4, \\ \qquad\qquad 0\le c < T_{\text{ZP}},\ \forall t\neq 0 \\ \dfrac{T_u - T_{\text{ZP}}}{T_s}\left(\sum_{l=0}^{L-1}|h(l)|^2\sigma_x^2 + \sigma_n^2\right)^2 \\ \quad + \dfrac{2T_{\text{ZP}}}{T_s}\sigma_n^2\left(\sum_{l=0}^{L-1}|h(l)|^2\sigma_x^2 + \sigma_n^2\right), \\ \qquad\qquad \text{otherwise} \end{cases} \tag{17}$$

with μ_x^4 the fourth order moment of the transmitted signal and μ_n^4 the fourth order moment of the AWGN. The first term of (17) is the peak value of the power autocorrelation function at delay $k = 0$. For the second term of (17), the values of the power autocorrelation function for which k lies in the interval $0 \le c = |k - tT_s| < T_{ZP}$ for all $t \neq 0$ correspond to the values of periodic triangular functions, that is, values where the zero padding of the received power sequence and its shifted version overlap. The last term of (17) correponds to the values of k where the zero padding of the received power sequence and its shifted version do not overlap. We can observe that the phase and frequency offsets do not affect the power autocorrelation feature as the exponentials are canceled owing to the conjugate operation. Figure 5 shows the power autocorrelation (where the received power has been normalized to unity) for a received sequence of 10 ZP-OFDM symbols having WiMedia parameters [16] with an SNR of 5 dB on a CM-4 channel model [14]. We can also observe that the power autocorrelation varies periodically with a triangular shape function according to the symbol duration and the zero padding duration. The time difference between two consecutive triangles is actually the symbol duration T_s of the ZP-OFDM signal. To find the number of periods k_{opt} in the power autocorrelation function, we define the vector $\mathbf{d} = [d(0) \cdots d(N-1)]$ and its frequency transform $\mathbf{D} = \text{FFT}(\mathbf{d})$, and we compute

$$k_{opt} = \max_{k \neq 0} |\mathbf{D}(k)|^2. \tag{18}$$

Without loss of generality, the sampling period of the lowpass filter T_r is normalized to unity, leading to the estimated symbol duration:

$$T_s = \frac{N}{k_{opt}}. \tag{19}$$

The power autocorrelation has the shape of a pulse train convolved with a triangular function (as seen on Figure 5). To estimate the zero padding duration T_{ZP}, we build a target filter that best matches the received power autocorrelation. We assume that the received power has been normalized to unity knowing the estimate of the signal power p and the estimate of the oversampling factor q. The estimate of the received power can be written as

$$p = \frac{T_u}{T_s}\left(\sum_{l=0}^{L-1} |h(l)|^2 \sigma_x^2 + \sigma_n^2\right) + \frac{T_{ZP}}{T_s}\sigma_n^2. \tag{20}$$

We define the normalized power autocorrelation $\mathbf{d}^{norm}$ as the ratio between the power autocorrelation $\mathbf{d}$ and the square of the received power p. Considering only the development of the useful terms in (17), we can factorize the normalized power autocorrelation with periodic triangular functions depending only on the overlap between the received power sequence and its shifted version, symbol duration, useful time interval, and zero padding duration:

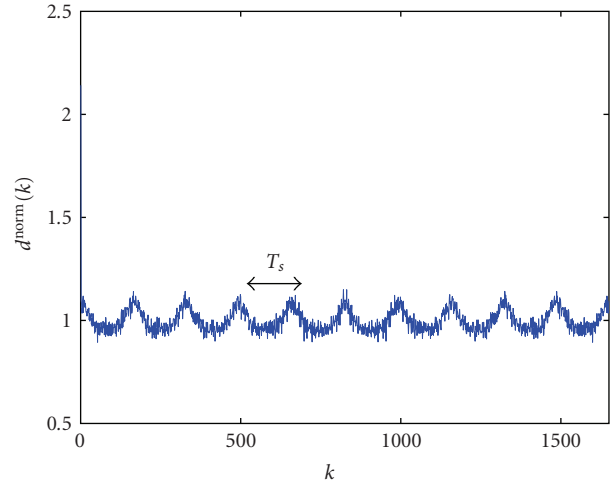

Figure 5: Power autocorrelation of a ZP-OFDM signal on a CM-4 channel model with SNR = 5 dB.

$$d^{norm}(k) = \begin{cases} \dfrac{T_u}{p^2 T_s}\left(\sum_{l=0}^{L-1} |h(l)|^4 \mu_x^4 + 4\sigma_x^2\sigma_n^2 + \mu_n^4\right) + \dfrac{T_{ZP}}{p^2 T_s}\mu_n^4, \\ \qquad k, t = 0, \\ \dfrac{(T_u - c)T_s}{T_u^2} \\ \quad \times \dfrac{1}{\left(1 + (T_{ZP}/T_u)(\sigma_n^2/(\sum_{l=0}^{L-1}|h(l)|^2\sigma_x^2 + \sigma_n^2))\right)^2} \\ \quad + \dfrac{2c}{p^2 T_s}\sigma_n^2\left(\sum_{l=0}^{L-1}|h(l)|^2\sigma_x^2 + \sigma_n^2\right) \\ \quad + \dfrac{T_{ZP} - c}{p^2 T_s}\sigma_n^4, \\ \qquad 0 \le c < T_{ZP},\ \forall t \neq 0, \\ \dfrac{(T_u - T_{ZP})T_s}{T_u^2} \\ \quad \times \dfrac{1}{\left(1 + (T_{ZP}/T_u)(\sigma_n^2/(\sum_{l=0}^{L-1}|h(l)|^2\sigma_x^2 + \sigma_n^2))\right)^2} \\ \quad + \dfrac{2T_{ZP}}{p^2 T_s}\sigma_n^2\left(\sum_{l=0}^{L-1}|h(l)|^2\sigma_x^2 + \sigma_n^2\right), \\ \qquad \text{otherwise.} \end{cases} \tag{21}$$

In order to calculate the surface under the triangular function, we shift the minimum of the power autocorrelation function to zero. Considering a target filter $\mathbf{d}_i^{target}$ with a zero padding of length i, the distance between the peaks and the minimum of the power autocorrelation function is $l_1 = T_s i/(T_s - i)^2$. We can also define the distance between the minimum of the power autocorrelation function and the

zero axis $l_2 = T_s(T_s - 2i)/(T_s - i)^2$. Therefore, the surface of the power autocorrelation shifted by l_2 ($\mathbf{d}^{\text{shifted}} = \mathbf{d}^{\text{norm}} - l_2$) is defined as

$$A_i = \sum\left(\mathbf{d}^{\text{norm}} - T_s\frac{T_s - 2i}{(T_s - i)^2}\right). \tag{22}$$

We design a target filter (using dec $= [0, 1/i, 2/i, \ldots, 1]$ and decr $= [1, \ldots, 2/i, 1/i, 0]$) as follows:

$$\mathbf{d}_i^{\text{target}} = \left[\frac{A_i}{ik_{\text{opt}}}(\text{ones}(i) - \text{dec}), \text{zeros}\left(\frac{N}{k_{\text{opt}}} - 2i\right), \frac{A_i}{ik_{\text{opt}}}(\text{ones}(i) - \text{decr})\right]^T \times k_{\text{opt}}. \tag{23}$$

The zero padding duration is then defined as $T_{\text{ZP}} = i_{\text{opt}}$ in the following optimization problem:

$$i_{\text{opt}} = \min_i\left(\mathbf{d}^{\text{shifted}} - \mathbf{d}_i^{\text{target}}\right)^2. \tag{24}$$

An exhaustive search on i is performed to solve this optimization problem. If $i_{\text{opt}} = T_{\text{ZP}}$, then the estimator is consistent at high SNR. Indeed, if we consider $\sigma_x^2 \gg \sigma_n^2$, we obtain

$$d^{\text{shifted}}(k) = \begin{cases}\dfrac{T_s(T_{\text{ZP}} - c)}{T_u^2}, & 0 \le c < T_{\text{ZP}},\ \forall t \ne 0\\ 0, & \text{otherwise.}\end{cases} \tag{25}$$

Then, the surface of the power autocorrelation shifted by l_2 becomes

$$A_{T_{\text{ZP}}} = k_{\text{opt}}T_s\frac{T_{\text{ZP}}^2}{T_u^2} \tag{26}$$

and the target filter is

$$\mathbf{d}_{T_{\text{ZP}}}^{\text{target}} = \left[\frac{T_sT_{\text{ZP}}}{T_u^2}(\text{ones}(i) - \text{dec}), \text{zeros}\left(\frac{N}{k_{\text{opt}}} - 2i\right), \frac{T_sT_{\text{ZP}}}{T_u^2}(\text{ones}(i) - \text{decr})\right]^T \times k_{\text{opt}}. \tag{27}$$

At high SNR, we therefore obtain $\mathbf{d}^{\text{shifted}} = \mathbf{d}_{T_{\text{ZP}}}^{\text{target}}$. Note that a better estimator can be found with the knowledge of the noise variance σ_n^2 replacing the distance l_2 in (22) by the last equation of (21). This could be done, for instance by tracking a part of the received signal where no signal transmission occurs. However, as this paper focuses on totally blind estimators, we consider only the estimator at high SNR for simulation results. Finally, knowing the oversampling factor q and the useful time interval $T_u = T_s - T_{\text{ZP}}$, we can determine the number of subcarriers having the sampling period of the lowpass filter T_r normalized to unity:

$$N_c = \frac{T_u}{q}. \tag{28}$$

Table 1: SUI channel models.

SUI 1 channel			
	Tap 1	Tap 2	Tap 3
Delay (μs)	0	0.4	0.9
Power (dB)	0	−15	−20
K factor	4	0	0
Doppler (Hz)	0.4	0.3	0.5
SUI 4 channel			
	Tap 1	Tap 2	Tap 3
Delay (μs)	0	1.5	4
Power (dB)	0	−4	−8
K factor	0	0	0
Doppler (Hz)	0.2	0.15	0.25

Table 2: OFDM signal parameters.

Parameters	WiMAX	WiMedia
Bandwidth	10 MHz	528 MHz
N_c	256	128
Number of samples in $T_{\text{CP,ZP}}$	64	37
T_u	25.6 μs	242.42 ns
$T_{\text{CP,ZP}}$	6.4 μs	70.07 ns
Channels	SUI-1&4	CM1&4
Nb symbols	10	10

4. Results

Simulation results are performed on the Stanford University Interim (SUI) channel models [13] for WiMAX signals [17] and Ultra-Wideband (UWB) IEEE 802.15.4a Channels Models (CM) [14] for WiMedia signals [16]. Two types of channels are chosen, on one hand the SUI-1 and the CM-1 channel models which have a Line-of-Sight (LOS) property for flat terrain with light tree density and, on the other hand, the SUI-4 and the CM-4 channel models which have a Non-LOS property for hilly terrain with heavy tree density. The different characteristics of SUI channels models are given in Table 1. For the CM channel models we refer to [14]. The parameters used for the WiMAX (CP-OFDM) and the WiMedia (ZP-OFDM) transmitters are given in Table 2.

When using these channel models to evaluate existing modulation recognition procedures discriminating between single-carrier and multicarrier modulations based on mixed moments and fourth order cumulants [2–4], it is observed that the threshold values for the different features can vary greatly with the different channel models. Therefore, these algorithms are not suitable for the detection of an OFDM signal without a priori knowledge of the channel conditions. The detection algorithms presented in this paper, however, are not based on the search for a threshold in a particular scenario, but rather on jointly detecting/estimating OFDM parameters blindly as in [5–7, 9–11].

Figure 6 shows the autocorrelation peaks observed for a received sequence of 10 CP-OFDM symbols (WiMAX parameters) with an SNR of 0 dB, a frequency offset $\epsilon = 0.4$, and a phase offset $\phi = \pi/4$ on an SUI-4 channel model. As

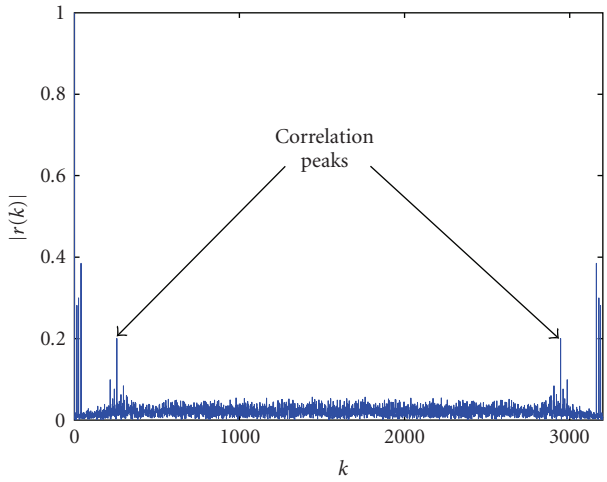

Figure 6: Autocorrelation of a CP-OFDM signal through SUI-4 channel model with AWGN at SNR = 0 dB.

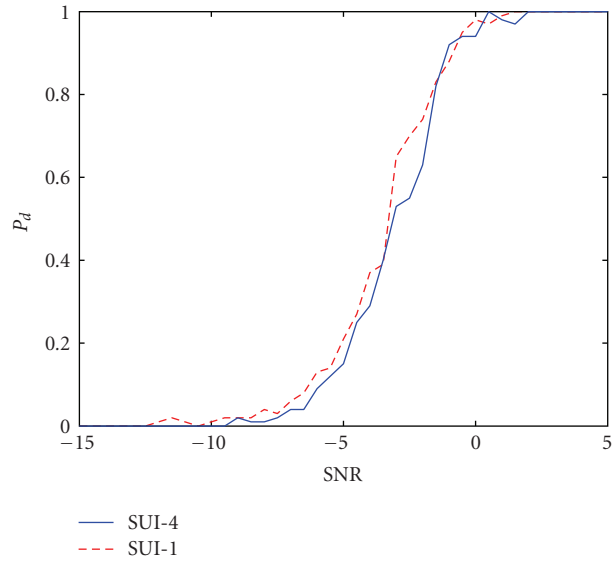

Figure 7: Probability of detection of a CP-OFDM signal through SUI-1&4 channels models with AWGN.

seen in [6, 7], the modulus of the autocorrelation feature is insensitive to phase and frequency offsets. We can see autocorrelation peaks at delay 0 and for short delays up to the maximum delay spread of the multipath channel. Then we can observe a significant peak corresponding to the useful time interval $T_u = 25.6$ microseconds (corresponding to a value 256 on the x-axis of the figure having normalized the sampling period of the lowpass filter T_r to unity). In this figure, two significant peaks can be observed owing to a cyclic shifting used in the autocorrelation operation.

Figure 7 shows the performance of the algorithm in terms of probability of correct detection (which indicates that the algorithm correctly estimates the useful time interval T_u and the CP duration T_{CP}) versus SNR (WiMAX parameters) on SUI-1&4 channel models. From this figure, we can conclude that at 5 dB we are sure to correctly estimate the useful time interval T_u and the CP duration T_{CP} of a CP-OFDM signal using a record of 10 OFDM symbols on generic SUI channel models. Moreover, the algorithm is rather insensitive to the channel (as good for SUI-4 as for SUI-1).

Figure 8 shows the Coefficient Variation Root Mean Square Deviation CV(RMSD) for the useful time interval T_u and the CP duration T_{CP} on SUI-1&4 channel models. The CV(RMSD) for the vector parameter $\boldsymbol{\theta}$ is defined as

$$\text{CV(RMSD)} = \frac{\sqrt{E\left[(\boldsymbol{\theta} - E[\boldsymbol{\theta}])^2\right]}}{E[\boldsymbol{\theta}]}. \tag{29}$$

The coefficient variation shows that the algorithms give a good estimate of the useful time interval T_u and the CP duration T_{CP} at a particular SNR threshold. On SUI-1 channel, the useful time interval T_u is well estimated at SNR $= -1$ dB, while its CP duration is well estimated at SNR $= 1$ dB. On SUI-4 channel, the useful time interval T_u is well estimated at SNR $= 0$ dB, while its CP duration T_{CP} is well estimated at SNR $= 2$ dB.

This characteristic can also be used for the detection of CP-OFDM signals. As the noise and the transmitted

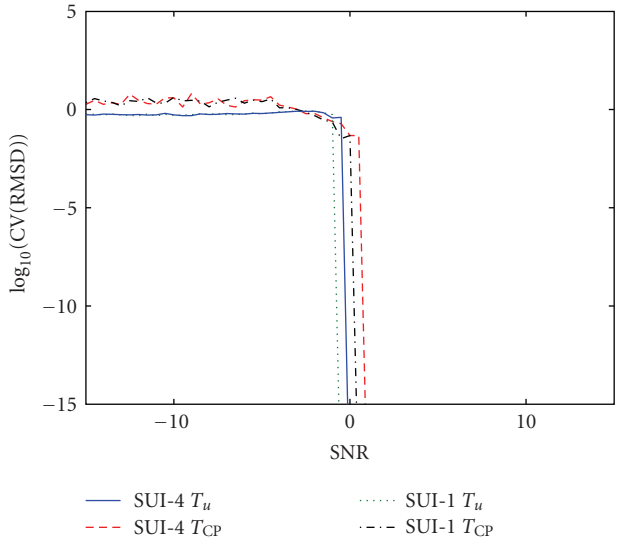

Figure 8: CV(RMSD) of the useful time interval T_u and the CP duration T_{CP} on SUI-1&4 channel models with AWGN.

sequence are random variables which are independent and identically distributed (i.i.d), the autocorrelation function of the received sequence is 0 for $k > L$. Moreover, the probability of false alarm for noise and single carrier modulations is related to the length of the window used for estimation $P_{\text{fa}} = 2/(N - 2L)$. In our simulations, we use a received sequence (which is referred as a "block") of 3200 samples (equivalent to the number of samples for 10 CP-OFDM WiMAX symbols) and a maximum number of channel taps $L = 60$, giving a probability of false alarm $P_{\text{fa}} = 6.49 \times 10^{-4}$. Consecutive blocks for noise and single carrier modulations will have a very high probability to give different estimates, while CP-OFDM signals will provide the same estimate with a very high probability. Therefore, if two consecutive

Table 3: Estimated parameters for CP-OFDM signals using real data measurements.

Data sets	GW26	GW24	GW22	GW20	GW18	GW16
q	5.1	5.6	6.2	6.5	7.3	8.2
p	0.12	0.15	0.17	0.19	0.22	0.27
T_u	127	127	127	127	127	126
T_s	145.5	145.5	145.5	145.5	142.9	145.5
N_c	24.9	22.7	20.5	19.5	17.4	15.5

blocks provide the same estimate of the useful time interval T_u or the CP duration T_{CP}, we declare that a CP-OFDM signal is detected. If the consecutive blocks provide different estimates of the useful time interval T_u or the CP duration T_{CP}, then the signal is declared either noise or single carrier modulation.

Table 3 shows the actual performance using a set of measured data similar to Figure 1 where the signal has already been downconverted to baseband. The data sets GW16-GW26 are CP-OFDM signals from 16 to 26 tones going through unknown channels and sampled at the receiver. The sampling period of the lowpass filter T_r is normalized to unity. This table shows that we can obtain a good approximation on the estimate of the number of subcarriers using real data measurements.

Figure 9 shows the shifted power autocorrelation variations for a received sequence of 10 ZP-OFDM symbols (WiMedia parameters) with an SNR of 0 dB and the target filter used for the estimation of the zero padding duration T_{ZP} given in (21) with a frequency offset $\epsilon = 0.4$ and a phase offset $\phi = \pi/4$ on a CM-4 channel model. As seen in Section 3, the power autocorrelation feature is insensitive to phase and frequency offsets. We can see that the succession of triangular functions can be well approximated by the target filter. However, the noise has a negative impact on the estimation of the zero padding duration, and therefore a significant SNR is necessary to have an accurate estimation of the zero padding duration T_{ZP} (cf. Figure 5 with SNR = 5 dB).

Figure 10 shows the performance of the power autocorrelation to estimate the symbol duration T_s for different values of the SNR (WiMedia parameters) on CM-1&4 channel models. The algorithm shows very good performance even at low SNR for 10 received ZP-OFDM symbols on generic Ultra-Wideband (UWB) IEEE 802.15.4a channel models, with very high probability of correct detection (which indicates that the algorithm correctly estimates the symbol duration T_s) at SNR = 5 dB. Moreover, if we use the power autocorrelation technique with 10 ZP-OFDM symbols and WiMAX parameters on SUI-1&4 channel models, we get a high probability of correct detection at SNR = 0 dB as seen on Figure 11, owing to the larger number of subcarriers $N_c = 256$ (or useful time interval $T_u = 25.6$ microseconds) and zero padding duration $T_{\text{ZP}} = 6.4$ microseconds compared to the WiMedia parameters. It can be shown by simulation that the key parameters are the number of subcarriers N_c (or useful time interval T_u), zero padding duration T_{ZP}, and number of OFDM symbols (the algorithm is rather

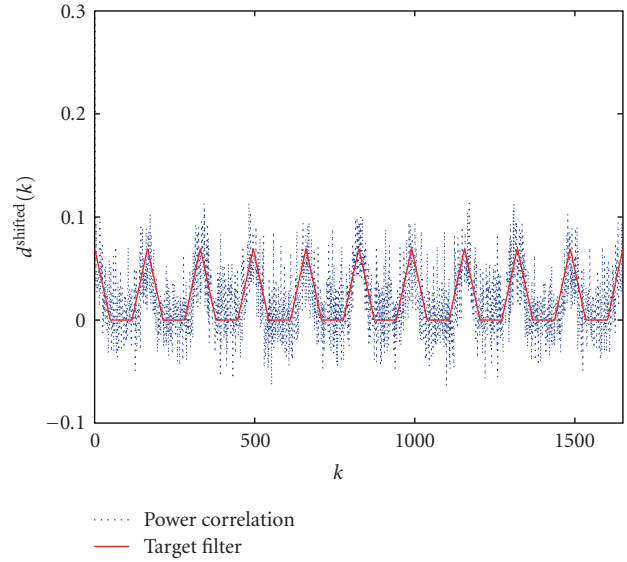

Figure 9: Power autocorrelation of a ZP-OFDM signal and its estimated target filter through CM-4 channel models with AWGN at SNR = 0 dB.

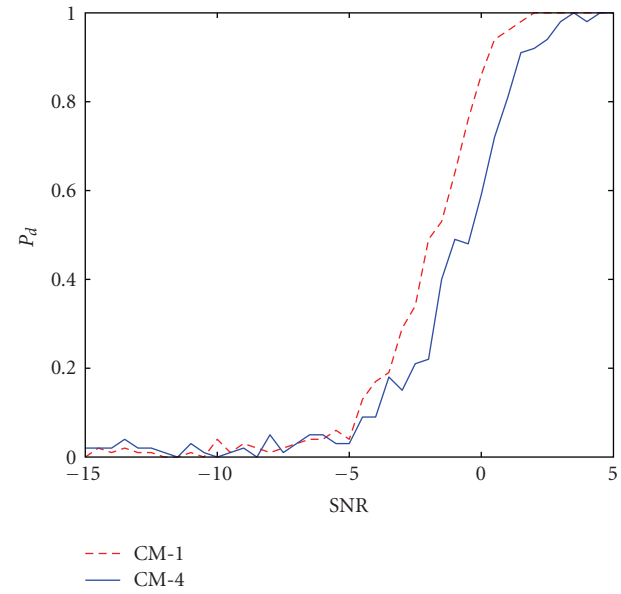

Figure 10: Probability of detection of a ZP-OFDM signal through CM-1&4 channel models with AWGN.

insensitive to the channel). In fact, the greater these key parameters, the lower the SNR necessary to achieve a perfect symbol duration detection.

Figure 12 shows the CV(RMSD) for the symbol duration T_s and the ZP duration T_{ZP} on SUI-1&4 channel models. The CV(RMSD) shows that the algorithms give a good estimate of the symbol duration T_s at a low SNR threshold. On SUI-1 channel, the symbol duration T_s is well estimated at SNR = 0 dB, while on SUI-4 channel, the symbol duration T_s is well estimated at SNR = 1 dB. As the zero padding duration T_{ZP} is more sensitive to noise, the

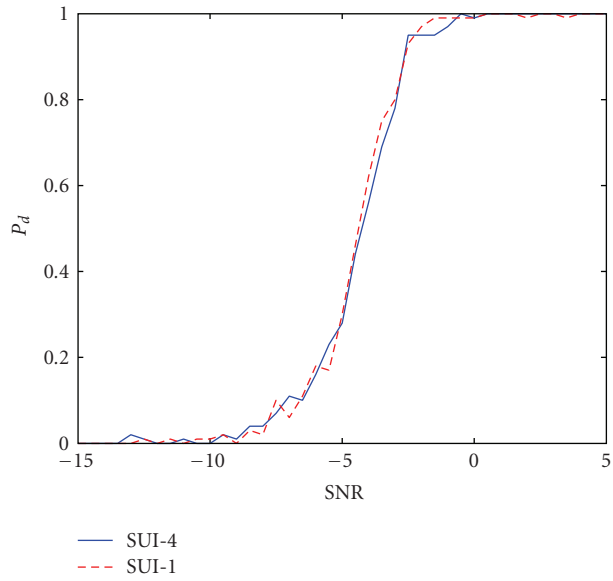

Figure 11: Probability of detection of a ZP-OFDM signal SUI-1&4 channel models with AWGN.

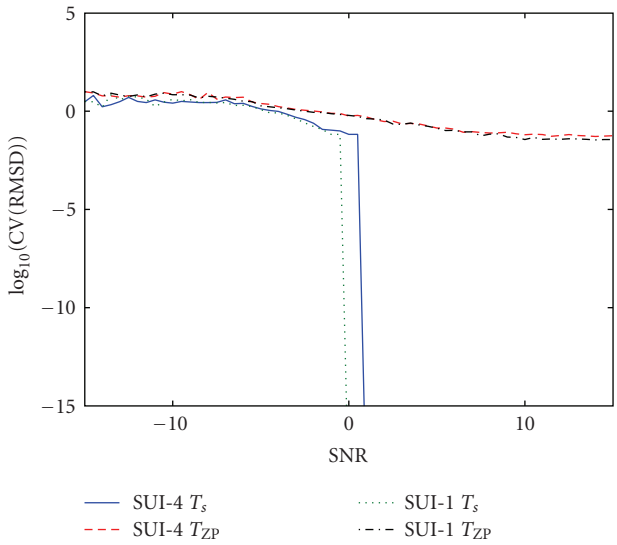

Figure 12: CV(RMSD) of the symbol duration T_s and the ZP duration T_{ZP} on SUI-1&4 channel models with AWGN.

CV(RMSD) for T_{ZP} reduces as the SNR increases. If we have to consider a feature for the detection of ZP-OFDM signals, the choice of T_s is more appropriate. Indeed, as the noise and the transmitted sequence are random variables which are independent and identically distributed (i.i.d), the shifted power autocorrelation function (25) of the received sequence is 0. Moreover, the probability of false alarm for noise and single carrier modulations is related to block size of the received sequence used for estimation $P_{fa} = 1/N$. In our simulations, we use a block of 1650 samples for WiMedia parameters and a block of 3200 samples for WiMAX parameters (equivalent to the number of samples for 10 ZP-OFDM symbols), giving a probability of false alarm $P_{fa} = 6.06 \times 10^{-4}$ and $P_{fa} = 3.13 \times 10^{-4}$, respectively. Consecutive blocks for noise and single carrier modulations will have a very high probability to give different estimates, while ZP-OFDM signals will provide the same estimate with a very high probability. Therefore, if two consecutive blocks provide the same estimate of the symbol duration T_s, we declare that a ZP-OFDM signal is detected. If the consecutive blocks provide different estimate of the symbol duration T_s, then the signal is declared either noise or single carrier transmission.

5. Conclusion

In this paper, we have proposed a blind parameter estimation technique based on a power autocorrelation feature applying to OFDM signals using a Zero Padding time guard interval (ZP-OFDM) which in particular excludes the use of the autocorrelation- and cyclic autocorrelation-based techniques. The proposed technique has led to an efficient estimation of the symbol duration and zero padding duration in frequency selective channels and was insensitive to receiver phase and frequency offsets. Simulation results were given for WiMAX and WiMedia signals using realistic Stanford University Interim (SUI) and Ultra-Wideband (UWB) IEEE 802.15.4a channel models, respectively. Simulation results have shown that OFDM signals without a CP (as used in WiMedia) could be detected based on their zero padding without any loss in performance compared to similar CP-OFDM parameter estimation algorithms. These techniques could be used in several applications to monitor ZP-OFDM signals and to estimate their parameters (Bluetooth 3.0, WiMedia, etc.).

Acknowledgment

This research work was carried out in the frame of the European FP7 UCELLS project. The scientific responsibility is assumed by its authors.

References

[1] O. Dobre, A. Abdi, Y. Bar-Ness, and W. Su, "Survey of automatic modulation classification techniques: classical approaches and new trends," *IET Communications*, vol. 1, no. 2, pp. 137–156, 2007.

[2] B. Wang and L. Ge, "Blind identification of OFDM signal in rayleigh channels," in *Proceedings of the 5th International Conference on Information, Communications and Signal Processing (ICICS '05)*, pp. 950–954, 2005.

[3] W. Akmouche, "Detection of multicarrier modulations using 4th-order cumulants," in *Proceedings of IEEE Military Communications Conference (MILCOM '99)*, vol. 1, pp. 432–436, 1999.

[4] D. Grimaldi, S. Rapuano, and L. de Vito, "An automatic digital modulation classifier for measurement on telecommunication networks," *IEEE Transactions on Instrumentation and Measurement*, no. 5, pp. 1711–1720, 2007.

[5] M. Öner and F. Jondral, "On the extraction of the channel allocation information in spectrum pooling systems," *IEEE Journal on Selected Areas in Communications*, vol. 25, no. 3, pp. 558–565, 2007.

[6] A. Punchihewa, O. Dobre, Q. Zhang, S. Rajan, and R. Inkol, "The n-th order cyclostationarity of OFDM Signals in time dispersive channels," in *Proceedings of the Asilomar Conference on Signals, Systems and Computers (ACSSC '08)*, August 2008.

[7] O. Dobre, A. Punchihewa, S. Rajan, and R. Inkol, "On the cyclostationarity of OFDM and single carrier linearly digitally modulated signals in time dispersive channels with applications to modulation recognition," in *Proceedings of IEEE Wireless Communications and Networking Conference (WCNC '08)*, pp. 1284–1289, Las Vegas, Nev, USA, 2008.

[8] H. Bolcskei, "Blind estimation of symbol timing and carrier frequency offset in wireless OFDM systems," *IEEE Transactions on Communications*, vol. 49, no. 6, pp. 988–999, 2001.

[9] H. Li, Y. Bar-Ness, A. Abdi, O. S. Somekh, and W. Su, "OFDM modulation classification and parameters extraction," in *Proceedings of the 1st International Conference on Cognitive Radio Oriented Wireless Networks and Communications (CROWNCOM '07)*, 2007.

[10] H. Ishii and G. W. Wornell, "OFDM blind parameter identification in cognitive radios," in *Proceedings of the 16th IEEE International Symposium on Personal, Indoor and Mobile Radio Communications (PIMRC '05)*, vol. 1, pp. 700–705, 2005.

[11] M. Shi, Y. Bar-Ness, and W. Su, "Blind OFDM systems parameters estimation for software defined radio," in *Proceedings of the 2nd IEEE International Symposium on New Frontiers in Dynamic Spectrum Access Networks (DySPAN '07)*, pp. 119–122, 2007.

[12] T. Yucek and H. Arslan, "Spectrum characterization for opportunistic cognitive radio systems," in *Proceedings of IEEE Military Communications Conference (MILCOM '06)*, 2006.

[13] IEEE 802.16 Broadband Wireless Access Working Group, "Channel models for fixed wireless application," IEEE 802.16a-03/01, 2003.

[14] A. F. Molisch, K. Balakrishnan, D. Cassioli, et al., "IEEE 802.15.4a Channel Model-Final Report," IEEE P802.15-04/662r0-SG4a, 2004.

[15] J.-J. van de Beek, M. Sandell, and P. O. Börjesson, "ML estimation of time and frequency offset in OFDM systems," *IEEE Transactions on Signal Processing*, vol. 45, no. 7, pp. 1800–1805, 1997.

[16] Standard ECMA-368, "High rate ultra wideband PHY and MAC standard," http://www.ecma-international.org/publications/files/ECMA-ST/ECMA-368.pdf.

[17] 802.16e-2005, "Air interface for fixed and mobile broadband wireless access systemsAmendment for physical and medium access control layers for combined fixed and mobile operation in licensed band," IEEE Standard, 2005.